



RESEARCH PAPER

# Maize 16-kD $\gamma$ -zein forms very unusual disulfide-bonded polymers in the endoplasmic reticulum: implications for prolamin evolution

Davide Mainieri,<sup>1</sup> Claudia A. Marrano,<sup>1</sup> Bhakti Prinsi,<sup>2</sup> Dario Maffi,<sup>2</sup> Marc Tschofen,<sup>3</sup> Luca Espen,<sup>2</sup> Eva Stöger,<sup>3</sup> Franco Faoro,<sup>2</sup> Emanuela Pedrazzini,<sup>1,\*</sup> and Alessandro Vitale<sup>1,\*</sup>

<sup>1</sup> Istituto di Biologia e Biotecnologia Agraria, CNR, 20133 Milano, Italy

<sup>2</sup> Dipartimento di Scienze Agrarie e Ambientali, Università degli Studi di Milano, 20133 Milano, Italy

<sup>3</sup> Department of Applied Genetics and Cell Biology, University of Natural Resources and Life Sciences, Vienna, Austria

\*Correspondence: [vitale@ibba.cnr.it](mailto:vitale@ibba.cnr.it) or [pedrazzini@ibba.cnr.it](mailto:pedrazzini@ibba.cnr.it)

Received 18 May 2018; Editorial decision 25 July 2018; Accepted 25 July 2018

Editor: Chris Hawes, Oxford Brookes University, UK

## Abstract

In the lumen of the endoplasmic reticulum (ER), prolamin storage proteins of cereal seeds form very large, ordered heteropolymers termed protein bodies (PBs), which are insoluble unless treated with alcohol or reducing agents. In maize PBs, 16-kD  $\gamma$ -zein locates at the interface between a core of alcohol-soluble  $\alpha$ -zeins and the outermost layer mainly composed of the reduced-soluble 27-kD  $\gamma$ -zein. 16-kD  $\gamma$ -zein originates from 27-kD  $\gamma$ -zein upon whole-genome duplication and is mainly characterized by deletions in the N-terminal domain that eliminate most Pro-rich repeats and part of the Cys residues involved in inter-chain bonds. 27-kD  $\gamma$ -zein also forms insoluble PBs when expressed in transgenic vegetative tissues. We show that in *Arabidopsis* leaves, 16-kD  $\gamma$ -zein assembles into disulfide-linked polymers that fail to efficiently become insoluble. Instead of forming PBs, these polymers accumulate as very unusual threads that markedly enlarge the ER lumen, resembling amyloid-like fibers. Domain-swapping between the two  $\gamma$ -zeins indicates that the N-terminal region of 16-kD  $\gamma$ -zein has a dominant effect in preventing full insolubilization. Therefore, a newly evolved prolamin has lost the ability to form homotypic PBs, and has acquired a new function in the assembly of natural, heteropolymeric PBs.

**Keywords:** Cereal seeds, disulfide bonds, endoplasmic reticulum, genome-wide duplication, neofunctionalization, prolamins, protein bodies, protein evolution.

## Introduction

Prolamins are present only in the seeds of grasses, where they are usually the main proteins, and thus constitute the major global source of food protein (Shewry and Halford, 2002). Their most striking and unique cell biology feature is their accumulation within the lumen of the endoplasmic reticulum (ER) as very large heteropolymers, termed protein bodies (PBs; Shewry and Halford, 2002; Pedrazzini *et al.*, 2016). Most proteins that enter

the ER are destined to be secreted or sorted to distal locations of the endomembrane system, whereas ER residents, which are mainly folding helpers, have specific amino acid signals that allow their retention/retrieval in the ER (Gomez-Navarro and Miller, 2016). Since these signals are not present in prolamins, the question arises as to what are the molecular features that determine prolamin ER residence and ordered PB formation.

Maize (*Zea mays*) prolamins are divided into four classes:  $\alpha$ -zeins (>30 genes),  $\gamma$ -zeins (three genes), and  $\delta$ -zeins and  $\beta$ -zeins (both single genes; Woo *et al.*, 2001; Xu and Messing, 2008). 27-kD  $\gamma$ -zein and  $\beta$ -zein are the oldest maize prolamins (Xu and Messing, 2008). Whole-genome duplications (WGD), particularly common in plants (Jiao *et al.*, 2011), are followed by rearrangements that can lead to gene loss or retention. In the latter case, functional buffering or neofunctionalization can occur, and play important roles in evolution (Chapman *et al.*, 2006; Kassahn *et al.*, 2009). About 5–12 million years ago, maize underwent WGD followed by allotetraploidization (Swigoňová *et al.*, 2004). As a result,  $\gamma$ -zein, originally a single gene encoding a polypeptide of 27-kD and one of the most ancient maize prolamins, now has representatives in homologous regions of chromosome 7 (27- and 50-kD  $\gamma$ -zein; hereafter referred to as 27 $\gamma$ z and 50 $\gamma$ z) and chromosome 2 (16-kD  $\gamma$ -zein; 16 $\gamma$ z). 16 $\gamma$ z most probably originates from duplication of the 27 $\gamma$ z gene followed by deletion events (Xu and Messing, 2008).

During endosperm development,  $\gamma$ - and  $\beta$ -zeins are synthesized first, forming a PB where  $\alpha$ - and  $\delta$ -zeins will later accumulate (Lending and Larkins, 1989). In the mature PB,  $\beta$ -zein, 27 $\gamma$ z, and 50 $\gamma$ z form the outer layer in contact with the luminal face of the ER membrane, whereas  $\alpha$ - and  $\delta$ -zeins form the inner core, with 16 $\gamma$ z located at the interface between the core and the outer layer (Lending and Larkins, 1989; Yao *et al.*, 2016). Yeast two-hybrid data suggest that 16 $\gamma$ z can interact with zeins of all classes (Kim *et al.*, 2002, 2006). 27 $\gamma$ z expressed in vegetative tissues of transgenic plants forms homotypic PBs, indicating that no specific features of the maize endosperm ER are necessary to form a PB (Geli *et al.*, 1994). The primary sequence of 27 $\gamma$ z (Fig. 1) consists of the transient signal peptide for translocation into the ER (co-translationally removed), followed by a region containing eight or seven (depending on the maize variety) repeats of the hexapeptide PPPVHL and seven Cys residues involved in inter-chain bonds that make the protein insoluble in non-reducing conditions, and finally a second region homologous to 2S albumins, which are vacuolar storage proteins present in various amounts in all land plants (Vitale *et al.*, 1982; Prat *et al.*, 1985; Mainieri *et al.*, 2014). 2S albumins belong to a larger class characterized by the eight-cysteine motif, consisting of four intra-chain disulfide bonds between three helical domains (Pedrazzini *et al.*, 2016; Fig. 1). This motif is also conserved in 27 $\gamma$ z (Ems-McClung *et al.*, 2002). Progressive Cysto-Ser mutation of the seven Cys residues of the N-terminal region lead to increased solubility and a parallel increase in the ability to leave the ER along the secretory pathway (Mainieri *et al.*, 2014). When the N-terminal region including the first six Cys residues is fused at the C-terminus of phaseolin, the vacuolar 7S storage globulin of common bean, the chimeric protein zeolin formed homotypic PBs in the ER (Mainieri *et al.*, 2004). Zeolin was instead efficiently secreted upon *in vivo* treatment with a reducing agent, or when its six Cys residues were mutated to Ser (Pompa and Vitale, 2006). Overall, these studies indicate that the N-terminal region of 27 $\gamma$ z contains key information for PB assembly and that its Cys residues are necessary for this process.

16 $\gamma$ z is mainly characterized by the loss of large part of the N-terminal, Pro-rich domain and three of its seven Cys residues (Prat *et al.*, 1987; Fig. 1). Additionally, its C-terminal region has lost one Cys residue of the eight-cysteine motif and has acquired a new one near the C-terminus, resulting in a new CysProCys sequence. This tripeptide could form an intra-chain disulfide bond (Yu *et al.*, 2012); however, it is not known whether this occurs in 16 $\gamma$ z. The changes that have generated 16 $\gamma$ z are noteworthy, since Cys residues are rarely lost once acquired during evolution (Wong *et al.*, 2011; Feyertag and Alvarez-Ponce, 2017). 16 $\gamma$ z can thus provide information on the minimal requirements for PB biogenesis and the features that allow the formation of heteropolymeric maize PBs. Here, we show that, unlike 27 $\gamma$ z, ectopically expressed 16 $\gamma$ z remains in part soluble, mainly because of the mutations in the N-terminal region. 16 $\gamma$ z is unable to form PBs, but it stably accumulates as polymers that markedly enlarge the ER lumen, giving rise to very unusual filamentous structures. These characteristics indicate neofunctionalization after WGD and cast light on the molecular basis for the specific organization of maize PBs.

## Materials and methods

### Analysis of maize PBs

Seeds from *Zea mays* inbred line W64A, collected at 25 d post-pollination and stored at -80 °C, were homogenized in a mortar using 5 ml g<sup>-1</sup> ice-cold 100 mM Tris-Cl, pH 7.4, 1.0 mM EDTA (buffer H), 7% (w/w) sucrose, and cOmplete™ Protease Inhibitor Cocktail (Roche). After filtration through cheesecloth, the homogenate was loaded on two layers of 35% and 60% (w/w) sucrose in buffer H and centrifuged in a swinging rotor for 90 min at 4 °C, 78 900 g<sub>av</sub> (i.e. the average g calculated at the middle length of the tube). The 7% sucrose supernatant, the interface between 7% and 35% sucrose, and the interface between 35%, and 60% sucrose were collected. After denaturation in the presence of 1% SDS and 4% 2-mercaptoethanol (2-ME), proteins were analysed using 15% SDS-PAGE. As expected (Vitale *et al.*, 1982), zeins were at the interface between 35% and 60% sucrose, and hence this is termed the PB fraction. To treat PBs with different solvents, immediately after collection the PB fraction was first diluted with the same volume of buffer H and centrifuged for 10 min at 4 °C, 1500 g<sub>av</sub>. The PB pellet was then resuspended in one of the following solvents: (i) buffer H, 1% Triton X-100, 20 min, 4 °C; (ii) buffer H, 2 mM dithiothreitol (DTT), 20 min, 4 °C; (iii) buffer H, 4% 2-ME, 20 min, 4 °C; and (iv) 70% ethanol in H<sub>2</sub>O, 90 min, 25 °C. After each treatment, samples were centrifuged for 10 min at 4 °C, 1500 g, the pellet and supernatant were then denatured and analysed using 15% SDS-PAGE and staining with Coomassie Brilliant Blue. Protein Molecular Weight Markers (Fermentas, Vilnius, Lithuania) were used as molecular mass markers.

### Plasmid constructions

The pDHA vector containing the coding sequence of 27-kD  $\gamma$ -zein followed by the FLAG epitope DYKDDDDK (hereafter termed 27 $\gamma$ zf) has been described previously (Mainieri *et al.*, 2014). To construct a similarly tagged 16-kD  $\gamma$ -zein (16 $\gamma$ zf), a genomic fragment of *Z. mays* W64A comprising the coding and untranslated flanking sequences of 16-kD  $\gamma$ -zein (a kind gift from Angelo Viotti, CNR), identical to GenBank sequence EU953296.1, was amplified by PCR using the following oligonucleotides: 5'- ACTCAGGTCGAC**ATGAA** GGTGCTGATCGTTGCCCTTG -3' (where the Sall restriction site is in italics and the 16-kD  $\gamma$ -zein ATG start codon is in bold) and 5'- TCGATGGC**ATGCTCA**TTGTCGTCGTCCTTGTAGTCG

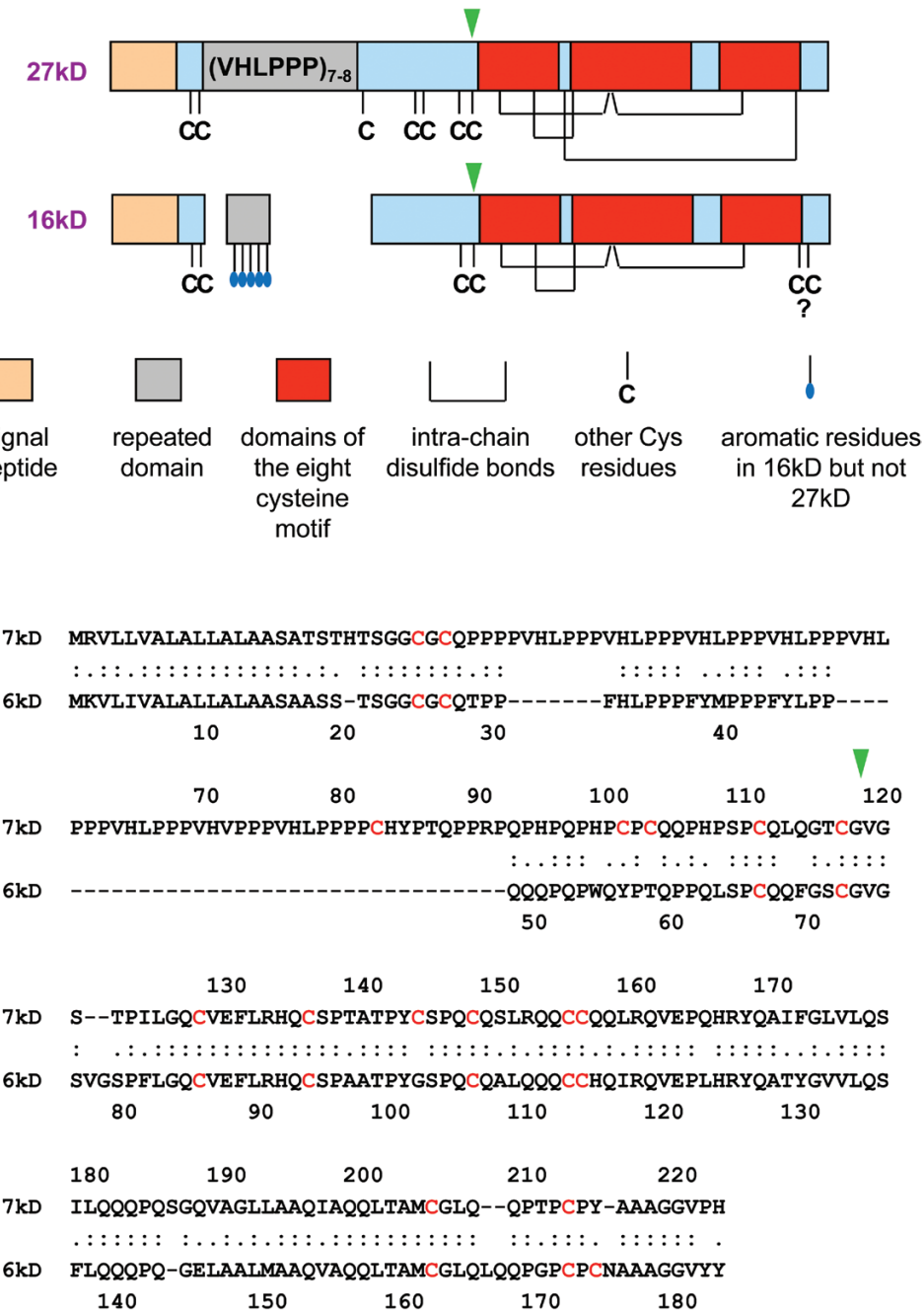


**Fig. 1.** Schematic diagram and amino acid sequence of the 27-kD and 16-kD  $\gamma$ -zein primary translation products. The question mark indicates that the linkage status of the two Cys residues towards the C-terminus of the 16-kD  $\gamma$ -zein is not known. The green arrowheads indicate the points at which the N- and C-terminal regions of the two polypeptides were exchanged, to produce constructs 27/16 and 16/27. In the amino acid sequences, Cys residues are highlighted in red.

TAGTAGACACCGCCGGCAGC -3', (where the SphI restriction site is in italics and the reverse complement of the codons encoding the FLAG epitope is underlined). The sequence was restricted with SalI and SphI and reinserted into the similarly restricted pDHA vector for transient expression.

To produce transgenic Arabidopsis, the EcoRI fragments containing the 16 $\gamma$ zf or 27 $\gamma$ zf expression cassettes were excised from pDHA and subcloned into EcoRI-linearized pGreenII0179 (John Innes Centre, Norwich, UK). The *Agrobacterium tumefaciens* strain GV3101 containing the pSoup helper plasmid was transformed with the resulting constructs.

To prepare the chimeric construct 16/27, which is formed by the N-terminal primary sequence of 16 $\gamma$ zf until Cys<sup>73</sup> followed by the C-terminal sequence of 27 $\gamma$ zf starting from Gly<sup>118</sup> (see Fig. 1), DNA was

synthesized (Integrated DNA Technologies, Leuven, Belgium) based on the two sequences and inserted into SalI/SphI restricted pDHA. To prepare the exactly reciprocal construct 27/16, the following DNA sequence was synthesized: from the Bpu10I restriction site of the sequence encoding 27 $\gamma$ zf until its Gly<sup>118</sup> codon (which corresponds to Gly<sup>74</sup> of 16 $\gamma$ zf), continuing with the 16 $\gamma$ zf sequence from Val<sup>75</sup> until its stop codon, and ending with a SphI restriction site. This sequence was used to substitute the Bpu10I/SphI fragment in pDHA encoding 27 $\gamma$ zf.

#### Transient expression in tobacco protoplasts

Transient expression was performed in protoplasts prepared from young (4–7 cm) leaves of tobacco (*Nicotiana tabacum* SR1) grown in axenic

conditions, as described previously (Mainieri *et al.*, 2014). Resuspensions of  $10^6$  protoplasts were transfected using 40 µg per million protoplasts of plasmid or, for co-transfections, 60 µg (25 µg of each plasmid plus empty pDHA to a final amount of 60 µg). After transfection and incubation for 20 h at 25 °C, protoplasts were either homogenized for protein blot analysis or subjected to pulse-chase labelling. Extraction of intracellular and secreted proteins in reducing or oxidizing conditions and protein blot analysis with rabbit anti-FLAG antibody (1:2000 dilution, Sigma-Aldrich) and the Super-Signal West Pico Chemiluminescent Substrate (Pierce Chemical, Rockford, IL) were performed as described previously (Mainieri *et al.*, 2014). Protein Molecular Weight Markers (Fermentas, Vilnius, Lithuania) were used as molecular mass markers.

Pulse-chase labelling was performed with 100 µCi ml<sup>-1</sup> Easytag mixture of <sup>35</sup>S-labelled Met and Cys (PerkinElmer) for 1 h at 25 °C. Chase was initiated by adding unlabelled Met and Cys to 10 mM and 5 mM, respectively. After incubation at 25 °C for the desired chase time, two volumes of ice-cold W5 buffer (Mainieri *et al.*, 2014) were added to each sample, which were then centrifuged at 60 g<sub>av</sub> for 10 min. Collected protoplasts and supernatant (containing secreted proteins) were homogenized with two volumes of ice-cold 150 mM NaCl, 1.5 mM EDTA, 1.5% Triton X-100, 150 mM Tris-Cl pH 7.5, supplemented with cComplete™ Protease Inhibitor Cocktail. After centrifugation at 10 000 g<sub>av</sub>, the pellet was resuspended in the same buffer supplemented with 4% 2-ME and centrifuged again. The soluble fractions of the first and second centrifugation were immunoselected using the anti-FLAG antibody and protein A Sepharose (GE Healthcare) and analysed using SDS-PAGE and radiography, using <sup>14</sup>C-methylated proteins (Sigma-Aldrich) as molecular mass markers. Radioactive proteins were detected using the Starion FLA-9000 Phosphoimage System (Fujifilm) and quantified using TotalLab Quant (TotalLab, Newcastle upon Tyne, UK).

#### Expression in transgenic *Arabidopsis*

Transgenic *Arabidopsis thaliana* (ecotype Columbia) plants expressing 16 $\gamma$ zf or 27 $\gamma$ zf were produced by the floral dip method (Clough and Bent, 1998) with the transformed *A. tumefaciens* described above. Hygromycin-resistant T0 plants were identified and the homozygous progenies were selected. Experiments were then conducted using T2 or T3 plants. Plants were grown in soil at 23 °C under a 16/8 h light/dark cycle or in sterile conditions on half-concentrated Murashige and Skoog media (Duchefa Biochemie) supplemented with 10 g L<sup>-1</sup> Sucrose and 0.8% (w/v) phyto agar (Duchefa Biochemie).

Leaves at 4–6 weeks old were homogenized in leaf homogenization buffer (150 mM Tris-Cl, pH 7.5, 150 mM NaCl, 1.5 mM EDTA, 1.5% Triton X-100, cComplete™ Protease Inhibitor Cocktail), supplemented (reducing conditions) or not (oxidizing conditions) with 4% (v/v) 2-ME. Soluble and insoluble proteins were separated by centrifugation at 1500 g<sub>av</sub> for 10 min at 4 °C. Samples were adjusted to 1.0% SDS, 4% 2-ME and analysed using SDS-PAGE followed by protein blotting with the anti-FLAG antibody (1:2000 dilution).

#### Subcellular fractionation

*Arabidopsis* leaves at 4–6 weeks old were homogenized in 10 mM KCl, 2 mM MgCl<sub>2</sub>, 100 mM Tris-Cl, pH 7.8 (buffer A), and 12% (w/w) sucrose at 4 °C, followed by isopycnic ultracentrifugation using linear 16–65% (w/w) sucrose gradients in buffer A as described previously (Mainieri *et al.*, 2004). Fractions of 650 µl were collected; 40 µl samples of each fraction were denatured and analysed by SDS-PAGE, followed by protein blotting with anti-FLAG antibody or rabbit anti-endoplasmic serum (Klein *et al.*, 2006; 1:2500 dilution).

To determine the solubility of  $\gamma$ -zeins present in the different subcellular fractions, fractions around either 1.19 or 1.29 density were frozen to break membranes and were then pooled. An equal volume of buffer A was added and the suspension was centrifuged at 1500 g<sub>av</sub> for 10 min, 4 °C. Supernatants (soluble proteins) were collected and denatured with SDS-PAGE denaturation buffer. Pellets were either resuspended in SDS-PAGE denaturation buffer or were further extracted with 70% ethanol in H<sub>2</sub>O for 90 min at 25 °C, and centrifuged at 1500 g<sub>av</sub> for 10 min, 25 °C.

The soluble fraction (ethanol-soluble) and insoluble pellet (ethanol-insoluble) were collected and denatured for SDS-PAGE.

#### Velocity sucrose-gradient ultracentrifugation

*Arabidopsis* leaves were homogenized in ice-cold leaf homogenization buffer. The homogenate was loaded on top of a linear sucrose gradient (150 mM NaCl, 1 mM EDTA, 0.1% Triton X-100, 50 mM Tris-Cl, pH 7.5, 5–25% [w/v] sucrose). After centrifugation at 200 000 g<sub>av</sub> for 20 h, 4 °C, equal volumes of each fraction were analysed using SDS-PAGE and protein blotting. An identical gradient loaded with molecular mass markers was run in parallel. For velocity ultracentrifugation in reducing conditions, leaf homogenization buffer was supplemented with 4% 2-ME, and the sucrose gradient buffer was supplemented with 2% DTT.

#### Electron microscopy

Tissue fragments (1–2 mm<sup>2</sup>) from fully expanded *Arabidopsis* leaves were fixed, embedded, and immunolabelled as previously described (Faoro *et al.*, 1991). Tissues were fixed in 1.2% glutaraldehyde and 3.3% paraformaldehyde in 0.1 M phosphate buffer, pH 7.4, at 4 °C for 2 h, post-fixed in 1% OsO<sub>4</sub> in the same buffer for 2 h, dehydrated in an ethanol series, and then embedded in Spurr's resin. For immunocytochemical localization, post-fixation was omitted and the embedding resin used was London Resin White. Immunolabelling was carried out on ultrathin sections mounted on nickel grids and incubated overnight at 4 °C with anti-FLAG antibody or, as a negative control, anti-Cucumber mosaic virus polyclonal antibody (DSMZ, Braunschweig, Germany), both at 1:1000 dilution. After washing, sections were incubated for 1 h at room temperature, with 15 nm gold-labelled goat anti-rabbit serum (1:20; British BioCell, Cardiff, UK) and stained with 2% uranyl acetate and lead citrate, before being examined with a 100SX TEM (Jeol, Japan) operating at 80 KV.

#### Fluorescence microscopy

Leaves from *Arabidopsis* plants grown for 2 weeks in soil were cut in half lengthwise and primary veins were removed. Staining was with 3,3'-dihexyloxocarbocyanine (DiOC6, Molecular Probes) at a concentration of 0.5 µg ml<sup>-1</sup> in PBS for 10 min, followed by washing three times in PBS. Small sections of stained leaves were placed on a microscope slide and visualized with a 63x oil immersion objective mounted on an Axiovert 200 microscope (Carl Zeiss) equipped for epifluorescence. Simultaneous visualization of DiOC6 stain (488 nm excitation/520 nm emission) and bright-field (visible lamp) was performed using the sequential scanning facility of the microscope. Images were assembled with Adobe Photoshop software 10.0.

## Results

#### A proportion of 16 $\gamma$ z present in maize PB is solubilized by alcohol

16 $\gamma$ z can be efficiently solubilized from maize endosperm by 70% ethanol supplied with reducing agent (Kim *et al.*, 2006), but its solubility in each of these agents alone is less clear. Treatment of purified PBs with buffer containing 2 mM DTT efficiently solubilizes 27 $\gamma$ z and 50 $\gamma$ z, but not PB polypeptides with molecular mass in the 16-kD range (Vitale *et al.*, 1982). We therefore examined in more detail the solubility of 16 $\gamma$ z accumulated in maize. An endosperm PB fraction prepared using a sucrose gradient was first treated with buffer containing 4% 2-mercaptoethanol (2-ME buffer, Fig. 2A). This reducing buffer solubilizes recombinant 27 $\gamma$ z (Mainieri *et al.*, 2014). The polypeptides that are underlined in Fig. 2 were identified

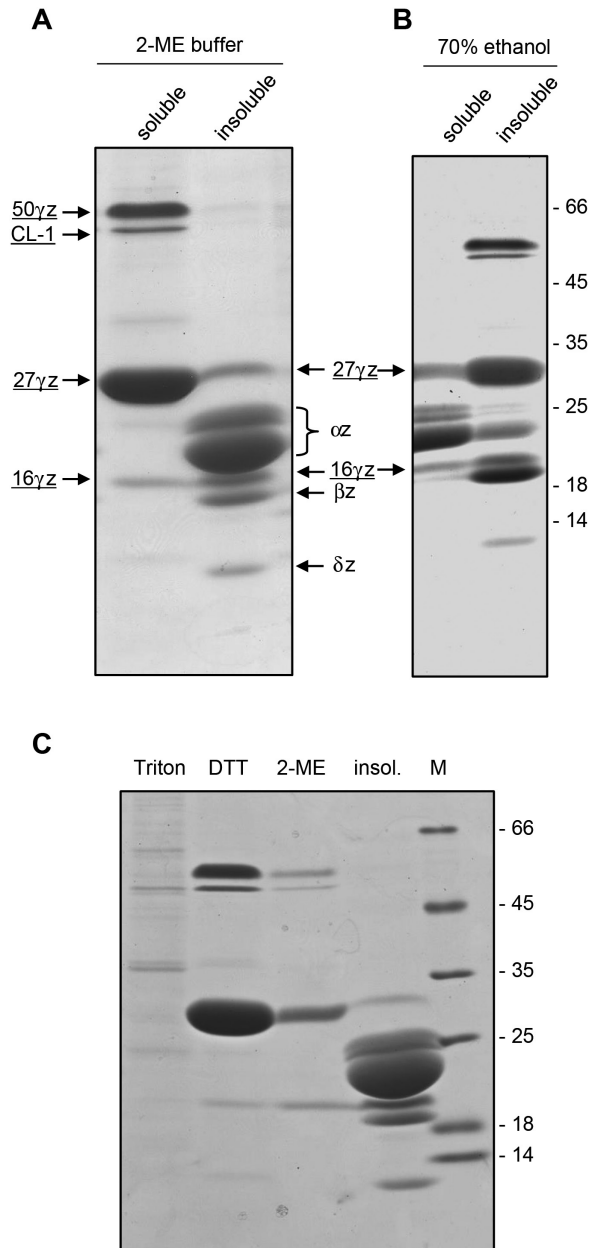


**Fig. 2.** The solubility of 16 $\gamma$ z accumulated in maize protein bodies (PBs) is intermediate between those of  $\alpha$ -zeins and the other  $\gamma$ -zeins. PBs purified from maize seeds, collected at 25 d after pollination, were treated at 4 °C with buffer containing 4% 2-ME (A) or at 25 °C with 70% ethanol in H<sub>2</sub>O (B). After centrifugation, soluble and insoluble proteins were analysed using SDS-PAGE and Coomassie staining. The different zein polypeptides ( $\alpha$ z,  $\beta$ z,  $\gamma$ z,  $\delta$ z) and CL-1 are indicated. Those whose identities were confirmed by LC-ESI-MS/MS are underlined (see Supplementary Fig. S1 and Supplementary Table S1). (C) Purified PBs were sequentially extracted with buffer containing 1% Triton X-100, 2 mM DTT, and 4% 2-ME. After each step, the suspension was centrifuged and the soluble material was analysed using SDS-PAGE and Coomassie staining, together with the insoluble material of the last extraction (insol.). The positions of molecular mass markers (M, in kD) are indicated to the right in (B) and (C).

by LC-ESI-MS/MS analysis (Supplementary Fig. S1 and its associated Methods, and Supplementary Table S1; 27 $\gamma$ z and 16 $\gamma$ z identities were confirmed in both the soluble and insoluble fractions); polypeptides without underlining indicate zeins

identified solely based on their typical SDS-PAGE migration rates (notice that prolamins migrate more slowly than expected from their sequences). The 2-ME buffer very efficiently solubilized 27 $\gamma$ z and 50 $\gamma$ z (Fig. 2A), as expected (Vitale *et al.*, 1982). In contrast, solubilization of 16 $\gamma$ z was only partial, with most of the protein remaining in the insoluble precipitate, unlike the two other  $\gamma$ -zeins (Fig. 2A).  $\alpha$ -zeins, which are alcohol-soluble (Misra *et al.*, 1976), were efficiently solubilized by 70% ethanol at 25 °C (Fig. 2B). In addition, a significant proportion of 16 $\gamma$ z was solubilized by ethanol, whereas 50 $\gamma$ z and 27 $\gamma$ z remained totally or almost totally insoluble (Fig. 2B). When PBs were sequentially extracted with buffer containing non-ionic detergent, 2 mM DTT (as in Vitale *et al.*, 1982) or 4% 2-ME, the results confirmed that  $\gamma$ -zeins are insoluble unless reduced and indicated that DTT was not more efficient than 2-ME in solubilizing 16 $\gamma$ z (Fig. 2C).

Minor amounts of corn legumin-1 (CL-1), an 11S storage globulin (Woo *et al.*, 2001; Yamagata *et al.*, 2003), were extracted using non-reducing buffer containing non-ionic detergent, but most of this protein was extracted in the presence of a reducing agent (Fig. 2A–C, Supplementary Fig. S1). 11S storage proteins usually accumulate in protein storage vacuoles, but the presence of CL-1 in PBs, especially at late stages of endosperm maturation, has been observed previously (Arcalis *et al.*, 2010; Reyes *et al.*, 2011).

The solubility of 16 $\gamma$ z accumulated in maize was therefore intermediate between that of  $\alpha$ -zeins and the other  $\gamma$ -zeins, and distinct from that of CL-1, and  $\beta$ - and  $\delta$ -zeins (these two minor zeins were not efficiently solubilized by either solvent, Fig. 2), indicating that 16 $\gamma$ z may have specific polymerization properties. We verified this by comparing the destinies of 16 $\gamma$ z and 27 $\gamma$ z expressed individually in plant cells.

#### Recombinant 16 $\gamma$ z and 27 $\gamma$ z are retained intracellularly but have different solubility

The 16 $\gamma$ z sequence was tagged at the C-terminus with the FLAG epitope. This construct (16 $\gamma$ zf) and similarly tagged 27 $\gamma$ z (27 $\gamma$ zf; Mainieri *et al.*, 2014) were first transiently expressed in tobacco protoplasts. SDS-PAGE and protein blotting with anti-FLAG antibody performed ~20 h after transfection indicated that 16 $\gamma$ zf was recovered intracellularly, with almost no sign of secretion (Fig. 3A). In addition to the expected abundant monomers, a small proportion of 16 $\gamma$ zf was detected as what appear to be dimers and larger oligomers, not disassembled by the denaturation buffer. Both the lack of secretion and the incomplete disassembly by the SDS-PAGE denaturing/reducing buffer were also characteristic of 27 $\gamma$ zf expressed in protoplasts (Fig. 3A, and see Mainieri *et al.*, 2014) and leaves of transgenic Arabidopsis (Geli *et al.*, 1994). Sequential extraction with non-reducing buffer and then buffer supplemented with 4% 2-ME indicated that 27 $\gamma$ zf was almost completely insoluble unless reduced (Fig. 3A, S2 fraction), as previously established (Mainieri *et al.*, 2014). A significant proportion of 16 $\gamma$ zf molecules was instead also soluble in the absence of reducing agent (Fig. 3A, S1 fraction), indicating inefficient formation of insoluble polymers. 70% ethanol did not solubilize either of the two constructs (Fig. 3B, SE fraction). When 27 $\gamma$ zf

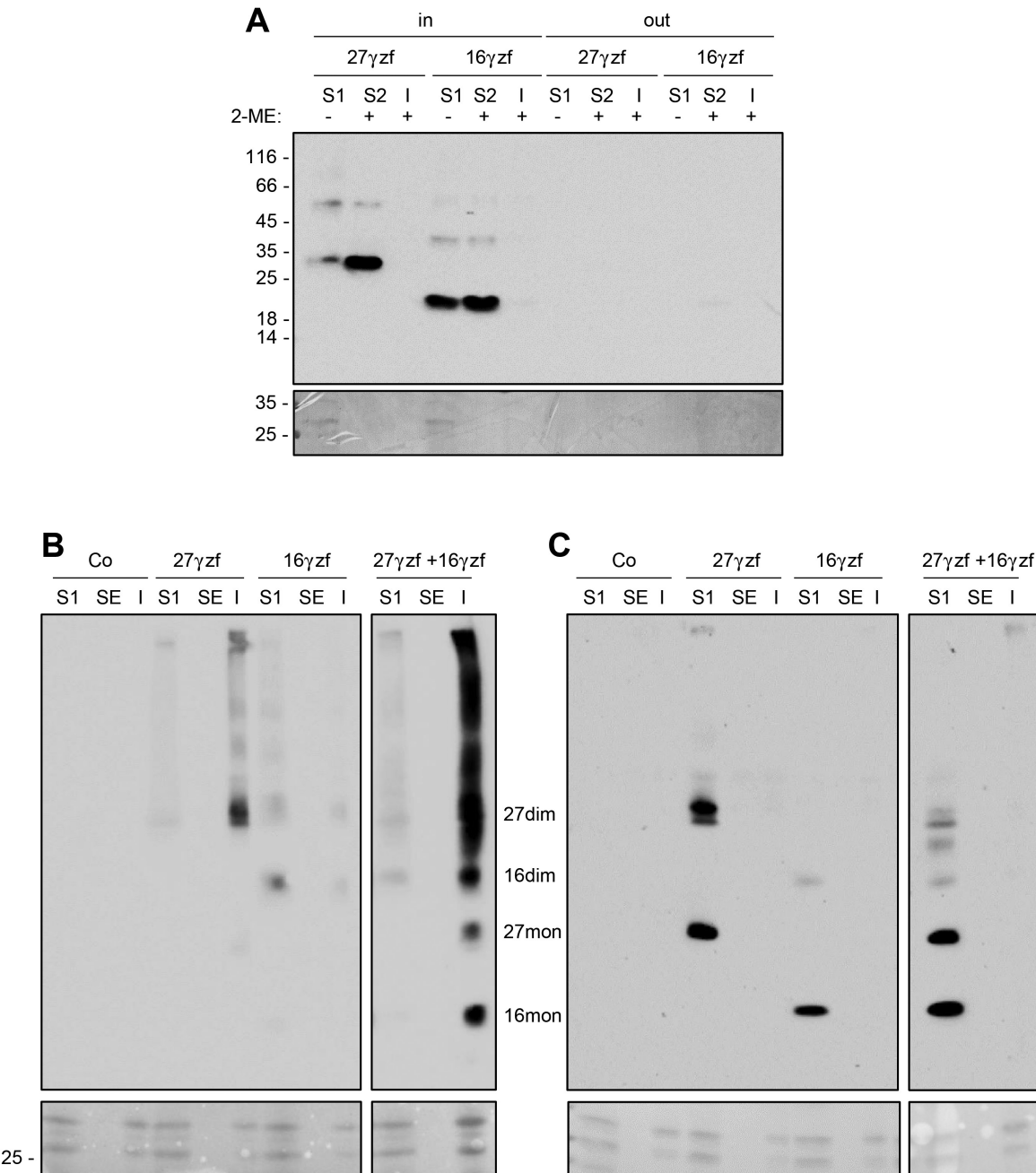


**Fig. 3.** Recombinant 16 $\gamma$ zf and 27 $\gamma$ zf are retained intracellularly but have different solubility. Protoplasts were isolated from tobacco leaves and transiently transformed either with plasmids encoding the indicated constructs or with the empty vector (Co) and analysed after incubation for 20 h. (A) Protoplasts (in) or incubation medium (out) were homogenized in the absence (–) of 2-ME. After centrifugation, soluble (S1) and insoluble fractions were collected. The insoluble material was resuspended in the presence (+) of 2-ME and subjected to a second centrifugation, to obtain the new soluble (S2) and insoluble (I) fractions. (B) Protoplasts were homogenized in the absence of 2-ME. After centrifugation, soluble (S1) and insoluble fractions were collected. The insoluble material was resuspended with 70% ethanol and subjected to a second centrifugation, to obtain the new soluble (SE) and insoluble (I) fractions. (C) As in (B), but the first homogenization was performed in the presence of 4% 2-ME. In (A–C), the upper images show analysis of each fraction by SDS-PAGE and protein blotting with anti-FLAG antibody, whilst the lower images show Ponceau S staining. The positions of molecular mass markers are shown to the left, in kD. In (B, C) the positions of dimers (dim) and monomers (mon) of 27 $\gamma$ zf (27) and 16 $\gamma$ zf (16) are indicated.

and 16 $\gamma$ zf were transiently co-expressed, both were almost completely insoluble in non-reducing buffer or 70% ethanol (Fig. 3B, I fraction). Therefore, the two  $\gamma$ -zeins interacted, and 27 $\gamma$ zf had a dominant effect in inhibiting 16 $\gamma$ zf solubility in the absence of reducing agent. When the first buffer of the sequential extraction was supplemented with 4% 2-ME, both individually expressed and co-expressed  $\gamma$ -zeins were fully

solubilized, confirming the role of disulfide bonds in determining insolubility (Fig. 3C, S1 fraction). These data were consistent with the insolubility of 16 $\gamma$ zf when natural maize PBs were treated with non-reducing buffer (see Fig. 2C) and suggested that its partial solubility in ethanol was due to interactions with  $\alpha$ -zeins. The relative proportions of monomers and oligomers detected by SDS-PAGE varied in independent experiments,

but their different solubility in non-reducing conditions, when individually expressed, was consistently observed (compare Fig. 3A and B, and see also Supplementary Fig. S2).

*In transgenic Arabidopsis, 16 $\gamma$ zf is mostly unable to assemble into subcellular structures with the typical PB density*

To compare the long-term destinies of the two zeins, the tagged constructs were expressed in transgenic Arabidopsis under a constitutive promoter. These plants did not show visually evident phenotypes or clear alterations in growth and reproduction. For each construct, accumulation in leaves varied in different independent transgenic plants, but the electrophoretic pattern was unaffected by the level of final accumulation (Fig. 4A). 16 $\gamma$ zf showed the same electrophoretic patterns whether extracted from transgenic leaves or transiently transfected protoplasts, while most 27 $\gamma$ zf monomers were clearly of higher apparent molecular mass in transgenic leaves (around 40 kD), with only a minor proportion migrating as in transient expression (around 30 kD; compare Figs 3A and 4A). This indicated 27 $\gamma$ zf-specific post-translational modifications that were not yet detectable during the first hours after synthesis, and that did not occur in maize seeds. Hydroxylation of proline residues is the most likely explanation, as previously observed (Geli *et al.*, 1994; Mainieri *et al.*, 2014).

Subcellular localization was first investigated by isopycnic ultracentrifugation of homogenates prepared in the absence of detergent, to maintain membrane integrity. 27 $\gamma$ zf accumulated mainly in structures with density around 1.29 (Fig. 4B). This is consistent with the known ability of 27 $\gamma$ z to form homotypic PBs in the absence of the other zeins (Geli *et al.*, 1994; Coleman *et al.*, 1996) and the known high density of zein or zeolin PBs in maize or transgenic plants (Larkins and Hurkman, 1978; Geli *et al.*, 1994; Mainieri *et al.*, 2004). Much lower amounts of 27 $\gamma$ zf, probably constituted by newly synthesized molecules not yet assembled into dense PBs, were recovered in lighter subcellular fractions that contain the ER resident endoplasmic (Klein *et al.*, 2006) and have the typical ER density (Fig. 4B). 16 $\gamma$ zf was similarly present in the two distinct subcellular fractions, but most of the protein was in this case in the endoplasmic-containing ER, suggesting a poor ability to form PBs (Fig. 4C).

To determine the solubility of 16 $\gamma$ zf or 27 $\gamma$ zf present at the two positions along the gradient, fractions around 1.19 or 1.29 density were pooled, extracted with buffer without reducing agent, and centrifuged to separate soluble and insoluble proteins. Around 50% of 16 $\gamma$ zf present in the less-dense fraction was solubilized by this treatment (Fig. 4D, S1), whereas nearly 100% of 16 $\gamma$ zf or 27 $\gamma$ zf present in fractions at 1.29 density was insoluble (Fig. 4D, P1). Treatment of P1 with 70% ethanol did not solubilize 16 $\gamma$ zf or 27 $\gamma$ zf (Fig. 4D, SE and PE; note that treatment with ethanol makes the denaturation of oligomers more difficult). We concluded that the relevant proportion of 16 $\gamma$ zf that was not assembled into dense subcellular structures was in part also soluble in the absence of reducing agent, but no 16 $\gamma$ zf molecules insoluble in aqueous buffer were alcohol-soluble. This strongly suggested that 16 $\gamma$ z in maize PBs

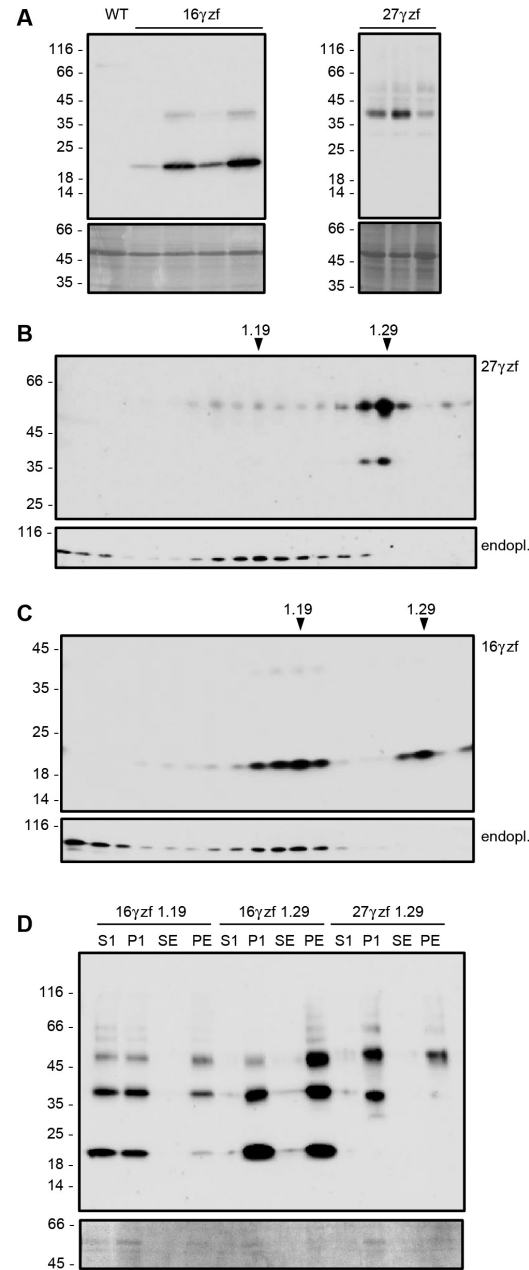


**Fig. 4.** Assembly of 16 $\gamma$ zf into dense subcellular structures is inefficient. (A) Leaves from transgenic Arabidopsis expressing 27 $\gamma$ zf or 16 $\gamma$ zf, or from wild-type plants (WT) were homogenized in the presence of 2-ME. Soluble proteins were analysed using SDS-PAGE. Each individual lane represents an independent transgenic plant. The upper images are protein blots with anti-FLAG antibody; lower images are Ponceau S staining. (B, C) Leaves from transgenic Arabidopsis expressing 27 $\gamma$ zf (B) or 16 $\gamma$ zf (C) were homogenized in the presence of 12% (w/w) sucrose and in the absence of detergent. The homogenates were fractionated by ultracentrifugation on 16–65% (w/w) isopycnic sucrose gradients. Proteins in each gradient fraction were analysed by SDS-PAGE and protein blotting, with anti-FLAG (27 $\gamma$ zf, 16 $\gamma$ zf) antibody or anti-endoplasmic (endopl.) serum. The top of gradients are at the left and the numbers at the top indicate the density ( $\text{g ml}^{-1}$ ). (D) Fractions around either 1.19 or 1.29 density from the gradients shown in (B, C) were pooled, extracted with buffer without reducing agent and centrifuged. Supernatants (S1) and pellets (P1) were collected. An aliquot of P1 was further treated with 70% ethanol and centrifuged to obtain ethanol-soluble (SE) and insoluble (PE) material. The upper image shows analysis by SDS-PAGE and protein blotting with anti-FLAG antibody; the lower image shows Ponceau S staining. In (A–D) the numbers at the left indicate the positions of molecular mass markers (kD).

is partially alcohol-soluble due to association with alcohol-soluble  $\alpha$ -zeins, as also suggested by the data in Fig. 3B.

When homogenates, prepared in non-reducing buffer supplemented with non-ionic detergent, were subjected to velocity sucrose-gradient ultracentrifugation, both 27 $\gamma$ zf and zeolin migrated at the bottom of tubes, indicating that they are large polymers (Mainieri *et al.*, 2004, 2014). Given the partial different subcellular localization and solubility of 16 $\gamma$ zf with respect of 27 $\gamma$ zf, we investigated whether 16 $\gamma$ zf also forms large polymers held together by disulfide bonds. Two plants accumulating different amounts of 16 $\gamma$ zf were analysed, to verify whether the expression levels influenced oligomerization (Fig. 5A). 16 $\gamma$ zf migrated to the bottom of the velocity ultracentrifugation tubes, independently of its level of accumulation (Fig. 5B, bottom panels). When leaf homogenization and velocity centrifugation were performed in reducing conditions, 16 $\gamma$ zf migrated in a position corresponding to monomers (Fig. 5B, top panels).

We concluded that 16 $\gamma$ zf forms extensive, disulfide-dependent polymers, in spite of its poor ability to form high-density subcellular compartments. We therefore used electron microscopy to compare the subcellular structures formed by 27 $\gamma$ zf and 16 $\gamma$ zf.

#### *16 $\gamma$ zf polymerizes into unusual reticular threads that markedly alter ER morphology*

In addition to typical ER membranes (Fig. 6A, ER, compare with wild-type tissue in 6D), 27 $\gamma$ zf leaf tissue showed electron-dense, round structures with diameters from a few hundred nanometres to more than one micron, with attached ribosomes (Fig. 6, PB). These structures, not present in wild-type plants, were labelled by anti-FLAG antibody (Fig. 6B, C), thus indicating that 27 $\gamma$ zf formed PBs. Homotypic PBs formed by recombinant 27 $\gamma$ z have been observed in *Arabidopsis* vegetative

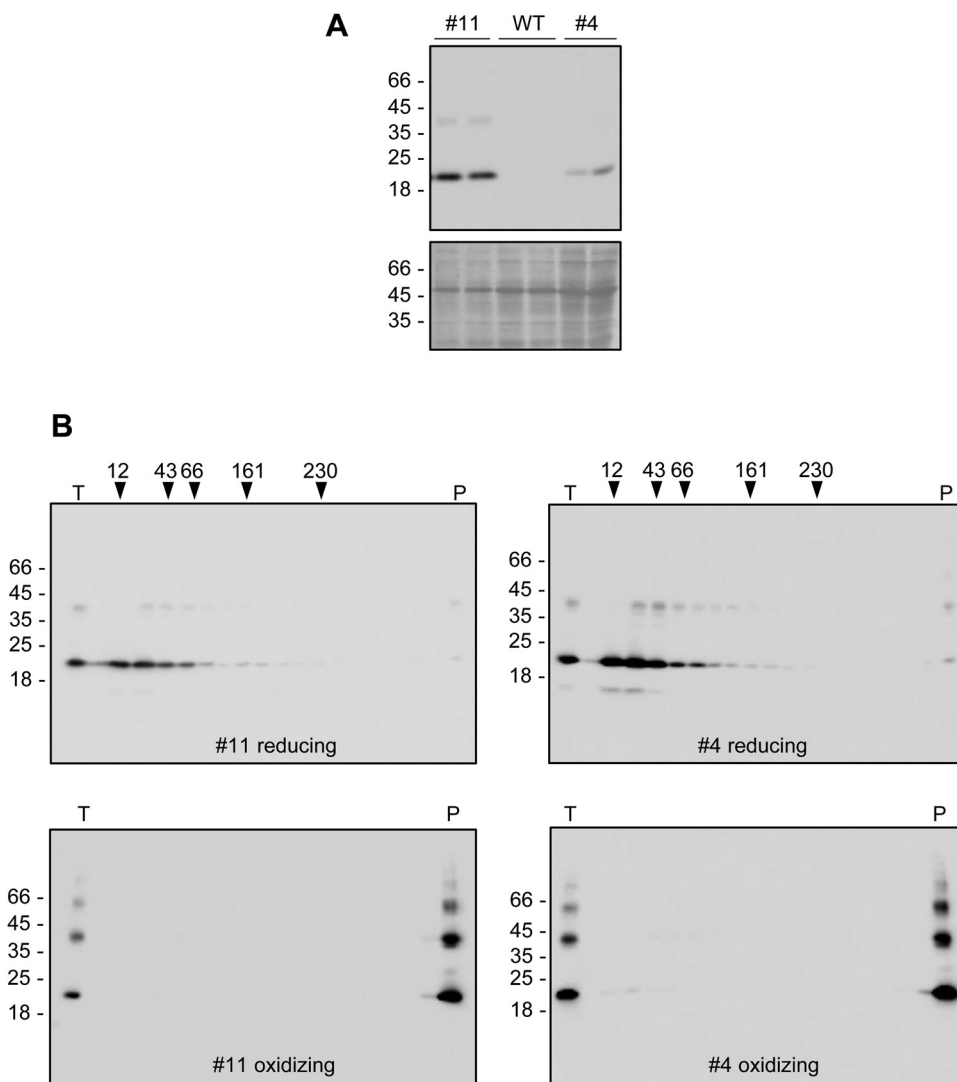


**Fig. 5.** 16 $\gamma$ zf forms large, disulfide-dependent polymers. (A) Homogenates were prepared from leaves of two independent transgenic *Arabidopsis* lines that accumulate different amounts of 16 $\gamma$ zf (#11 and #4, two plants for each line), and from leaves of untransformed wild-type *Arabidopsis* (WT), and analysed using SDS-PAGE. The upper image shows the protein blot with anti-FLAG antibody; the lower image shows Ponceau S staining. (B) Homogenates were prepared in either oxidizing or reducing buffer, and fractionated by velocity gradient ultracentrifugation. The top of each gradient is at the left. T, unfractionated total homogenate; P, pellet at the bottom of the tube after centrifugation. The numbers at the top indicate the positions where molecular mass markers migrate along the gradients. In (A, B) the numbers at the left indicate the positions of SDS-PAGE molecular mass markers (kD).

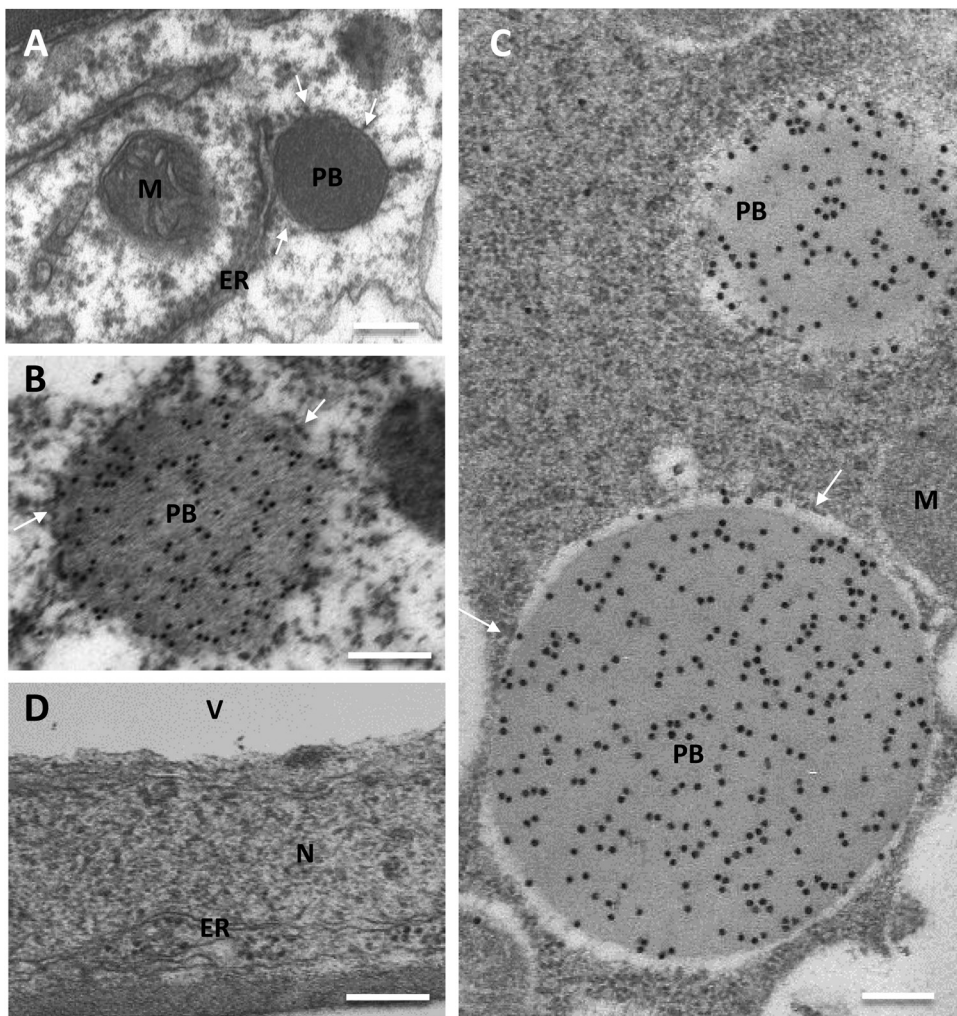


**Fig. 6.** 27 $\gamma$ zf forms protein bodies (PBs). Leaves from 6-week-old transgenic Arabidopsis plants expressing 27 $\gamma$ zf (A–C) or wild-type plants (D) were examined using electron microscopy. (A, D) Ultrathin sections post-fixed with osmium. (B, C) Immunolabelling with anti-FLAG antibody and secondary 15-nm gold-conjugated goat anti-rabbit serum. ER, endoplasmic reticulum; PB, protein body; M, mitochondria; N, nucleus, V, vacuole. Arrows indicate ribosomes. Note that in non-osmicated immunolabelled tissues (B, C) ER membranes are not detectable; however, numerous ribosomes are visible aligned outside the PB periphery (arrows). Scale bars are 200 nm.

tissues (Geli *et al.*, 1994) and tobacco seeds (Coleman *et al.*, 1996), although with smaller sizes than those that we observed.

Markedly different structures were formed by 16 $\gamma$ zf (Fig. 7). Large, irregular dilatations enclosed by a single membrane, often several micrometres wide, were detected (Fig. 7A; in Supplementary Fig. S3 black arrowheads mark the margins of this dilatation). The boundary membrane was surrounded by ribosomes (arrows in Fig. 7A, lower enlarged inset, and 7C, enlarged inset) and connections with tubular ER were occasionally seen (white arrowheads in Supplementary Fig. S3). The vacuole was often pressing against these dilatations, sometimes leaving space for a thin layer of cytoplasm outside the dilated ER (visible in the post-fixed sample in Fig. 7A, and more easily seen in Supplementary Fig. S3 where the ER membrane is indicated). The lumen of the ER dilatations contained very extensive electron-dense structures of two forms: very electron-opaque, osmiophilic threads of various lengths and irregular orientation (well represented in Fig. 7A, C) were mainly observed, whereas a minor proportion formed more compact irregular structures of lighter electron-density

(Fig. 7B, enlarged inset, and more evident in Fig. 7D, E). In non-osmicated tissues immunolabelled with anti-FLAG antibody, the convolutions appeared less sharp; however, gold particles were mostly aligned on them (Fig. 7B, D). No labelling occurred using an irrelevant antibody, confirming that the structures were formed by 16 $\gamma$ zf (Fig. 7E). The relative abundance of the two types of structures was variable in different ER dilatations, but when independent transgenic plants accumulating high (Fig. 7A, B, D, E) or low (Fig. 7C) amounts of 16 $\gamma$ zf were compared, no clear relationship between recombinant protein abundance and the type of 16 $\gamma$ zf structure could be established.

The ER vital lipophilic dye DiOC<sub>6</sub> also efficiently stains PBs in developing endosperm cells in both rice and maize, probably due to its high affinity for the hydrophobic prolamin polypeptides (Muensch *et al.*, 2000; Washida *et al.*, 2004). To complement the observations of electron microscopy, leaves were incubated with DiOC<sub>6</sub> and observed under conventional fluorescence microscopy (Fig. 8). In 16 $\gamma$ zf leaves, DiOC<sub>6</sub> highlighted enlarged structures of various sizes.

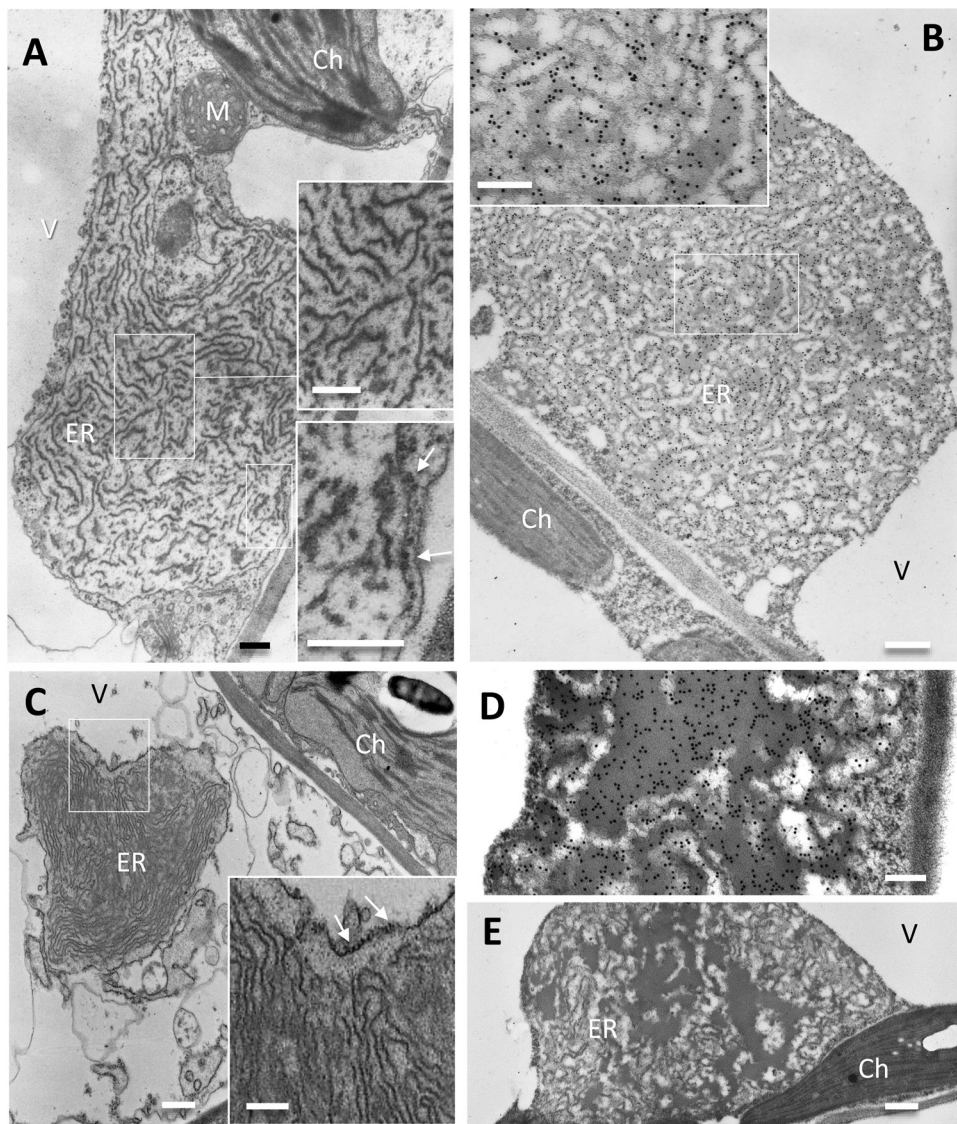


**Fig. 7.**  $16\gamma zf$  does not form protein bodies (PBs) but forms electron-dense structures in highly enlarged endoplasmic reticulum (ER) lumen. Leaves from 6-week-old transgenic *Arabidopsis* plants accumulating  $16\gamma zf$  in high (A, B, D, E) or low (C) amounts were analysed. (A, C) Ultrathin sections post-fixed with osmium. (B, D, E) Immunolabelling with anti-FLAG antibody (B, D) or irrelevant antibody as a negative control (E), and secondary 15-nm gold-conjugated goat anti-rabbit serum. The insets in (A-C) show magnifications to better illustrate the ribosomes attached on the cytosolic side of the ER membrane (arrows) and the electron-dense convoluted structures within the ER lumen. Ch, chloroplasts; M, mitochondria; V, vacuole. Scale bars in (B, C, E) are 200 nm; bars in (A, D) are 500 nm.

Higher magnification (Fig. 8A, inset, and magnification in 8D) showed that their content was not uniform, consistent with the structures observed by electron microscopy (Fig. 8D, arrow and compare with Fig. 7). In  $27\gamma zf$  leaves, more uniformly stained PBs with the classical size and round morphology were visible, as expected (Fig. 8G, and arrows in 8J). Structures similar to those in  $16\gamma zf$  and  $27\gamma zf$  were not detected in wild-type tissue, even at very high camera exposure times that highlighted the cell periphery, as expected for the ER lipophilic dye (Fig. 8M). Both the  $16\gamma zf$  structures and the  $27\gamma zf$  PBs were also detected under transmitted light (Fig. 8E, K, arrows).

We concluded that  $16\gamma zf$ , unlike  $27\gamma z$ , is unable to form PBs and instead polymerizes into novel electron-dense structures that mostly appear as irregular threads and cause marked enlargement of the ER lumen.

#### The N-terminal domain of $16\gamma z$ is responsible for the inefficient formation of insoluble polymers

To identify the structural features of  $16\gamma z$  that did not allow efficient formation of insoluble polymers, we measured the loss of solubility during pulse-chase labelling in transiently transfected tobacco protoplasts. After pulse labelling for 1 h with a mixture of [ $^{35}\text{S}$ ]Met and [ $^{35}\text{S}$ ]Cys, protoplasts were subjected to chase for 0, 4, or 8 h. At each time-point, protoplasts were directly extracted in reducing conditions (thus solubilizing all molecules of each construct, to measure synthesis and stability; Fig. 9A, B) or sequentially extracted: first in non-reducing buffer and then treating the insoluble material with reducing buffer (to calculate at each time-point the percentage of molecules that are insoluble unless reduced, Fig. 9C). Each extract was immunoselected with anti-FLAG antibody and analysed using SDS-PAGE

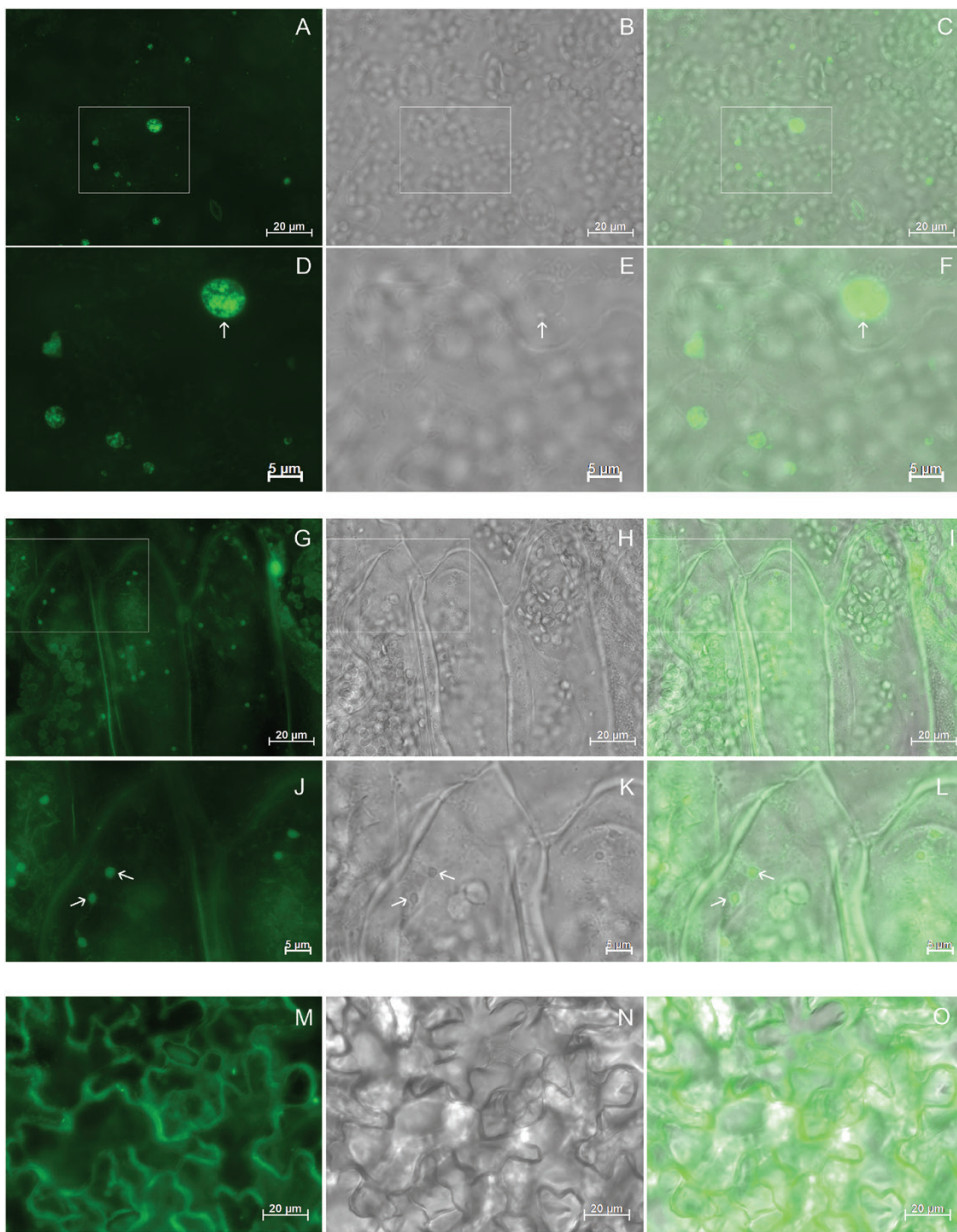


**Fig. 8.** 27 $\gamma$ zf protein bodies (PBs) and 16 $\gamma$ zf endoplasmic reticulum (ER) enlargements can be detected by fluorescence staining of the ER. Leaf tissue from 16 $\gamma$ zf (A–F), 27 $\gamma$ zf (G–L) or wild-type (M–O) Arabidopsis plants was stained with DiOC6 dye and examined using epifluorescence microscopy. (A, D, G, J, M): DiOC6 fluorescence (green); (B, E, H, K, N): bright-field; (C, F, I, L, O): merged images. Camera exposure time (ms): 61 (A), 502 (G), 8352 (M). Boxes in (A–C) and (G–I) indicate the regions that are shown at higher magnification in (D–F) and (J–L), respectively. Arrows indicate enlarged ER (D–F) or PBs (J–L).

and radiography. Newly synthesized 16 $\gamma$ zf and 27 $\gamma$ zf had the expected molecular mass (Fig. 9A). 16 $\gamma$ zf was slightly more stable during the chase (Fig. 9B; data are from two fully independent experiments). Already at the 0 h chase time-point, a much higher percentage of 27 $\gamma$ zf than 16 $\gamma$ zf was insoluble unless reduced (Fig. 9C). Insolubility increased during the chase, but the marked difference between the two zeins remained, as expected from the previous solubility assays (Figs 3, 4D). To map the insolubility determinant, we prepared two constructs, 27/16 and 16/27, in which the N-terminal domain of each zein was exchanged with that of the other (Fig. 1, the green arrowheads indicate the points of exchange). Since most of the molecular mass difference between the two zeins is due to their N-terminal

domain, the SDS-PAGE migrations of 27/16 and 16/27 are similar to those of 27 $\gamma$ zf and 16 $\gamma$ zf, respectively (Fig. 9A). The replacement of the natural N-terminal domain of 27 $\gamma$ zf with that of 16 $\gamma$ zf markedly inhibited insolubilization (Fig. 9C, compare 27 $\gamma$ zf and 16/27), whereas the reciprocal replacement markedly stimulated this process (Fig. 9C, compare 16 $\gamma$ zf and 27/16). This indicated that the N-terminal domain is the major determinant for the different behavior of the two zeins.

## Discussion

Mutations and insertions in the ancient seed storage proteins of the 2S albumin class were the first events in the origination of

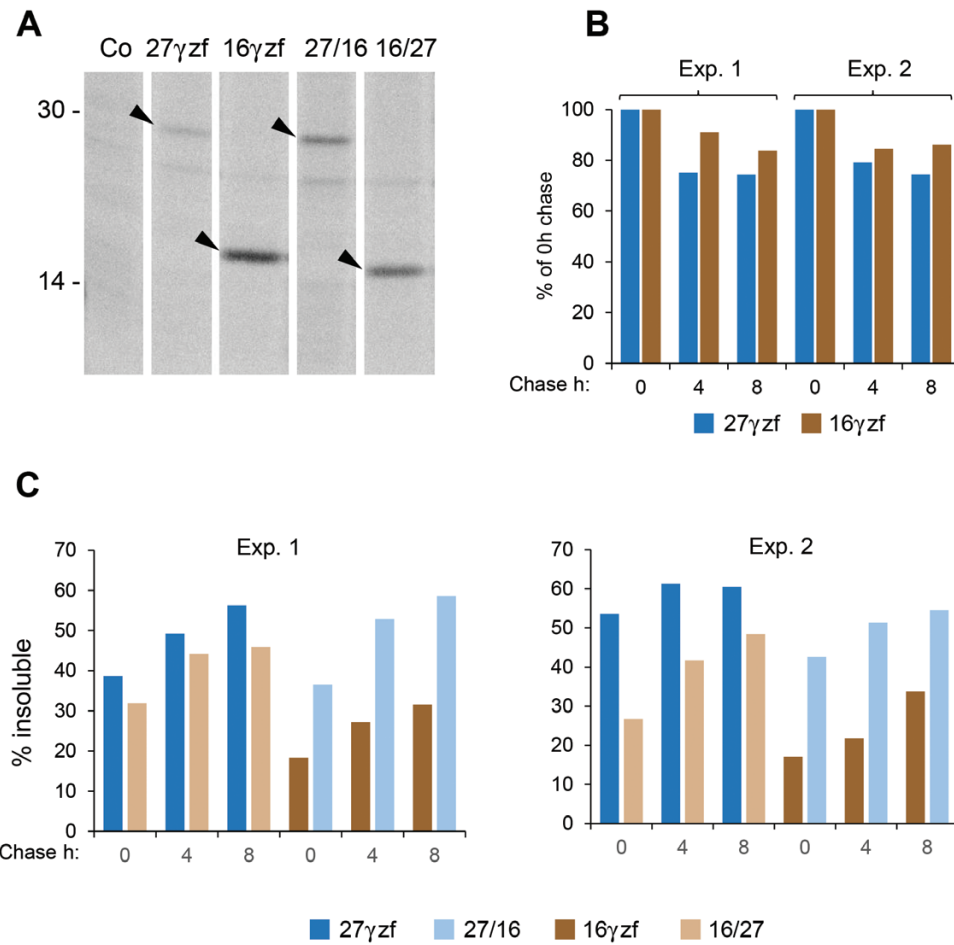


**Fig. 9.** The N-terminal domain of 16γzf has a major role in inhibiting the formation of insoluble polymers. Protoplasts prepared from tobacco leaves were transiently transfected either with plasmids encoding the indicated constructs or with empty plasmids (Co). (A) Transfected protoplasts were pulse-labelled with radioactive amino acids for 1 h before homogenization in reducing conditions. Proteins were immunoselected using anti-FLAG antibody and analysed using SDS-PAGE and radiography. The different lanes are from a single exposure of a single radiograph from which irrelevant lanes have been removed. The newly synthesized recombinant polypeptides (arrowheads) and the positions of molecular mass markers (numbers at left, kD) are indicated. (B) Protoplasts pulse-labelled as in (A) were subjected to chase for the indicated time (h), homogenized in the presence of 2-ME, immunoselected with anti-FLAG antibody, and analysed using SDS-PAGE and radiography. At each chase time-point, the densities of the relevant radioactive bands were quantified and expressed as percentage of the intensity at 0 h chase. (C) Protoplasts pulse-labelled as in (A) and chased for the indicated time (h) were then subjected to sequential homogenization steps, first in the absence 2-ME and then treating the insoluble material with 2-ME. Proteins at each step were immunoselected with anti-FLAG antibody and analysed using SDS-PAGE and radiography. At each time-point, the densities of the relevant radioactive bands were quantified and, for each construct, expressed as percentage in the second immunoprecipitation step divided by the sum of the two immunoprecipitations (% insoluble). In (B, C) values from two fully independent transient expression experiments are shown.

prolamins (Xu and Messing, 2009; Gu *et al.*, 2010; Pedrazzini *et al.*, 2016). This led to the assembly in PBs and a change in the subcellular compartment used for permanent accumulation from the vacuole to the ER, particularly in rice and pani-coid cereals such as maize, sorghum, and millet (Lending and Larkins, 1989; Shewry and Halford, 2002; Saito *et al.*, 2012).

16γzf originated upon maize WGD (Xu and Messing, 2008) and it is mainly characterized by deletions in the N-terminal region of 27γz, the most ancient γ-zein. We have shown here that recombinant 16γzf ectopically expressed in vegetative tissues accumulated within the ER, forming unusual structures. These did not resemble PBs or other ER-located polymers formed by natural or recombinant proteins expressed in plants (Bagga *et al.*, 1995; Mainieri *et al.*, 2004; de Virgilio *et al.*, 2008; Conley *et al.*, 2009; Saito *et al.*, 2009; Torrent *et al.*, 2009; Llop-Tous *et al.*, 2010). 16γzf structures mainly consisted of extensive, convoluted but well-defined filamentous threads; more

rarely, the enlarged ER also contained irregular, homogeneously electron-dense sectors, which may represent the proportion of 16γzf that had become insoluble. At the onset of prolamin accumulation, initial irregular dilatations along the ER have been observed in rice, but with diameters below 1 μm (Kawagoe *et al.*, 2005). 8S globulin, a mung bean vacuolar storage protein, forms 0.2–0.6 μm ER enlargements in transgenic tobacco BY2 cells and, as a GFP fusion, in Arabidopsis vegetative tissues and young developing seeds, to be correctly deposited in Arabidopsis storage vacuoles only at later seed development (Wang *et al.*, 2013). The sizes of these ER structures are one order of magnitude smaller compared the dilatations caused by 16γzf. Wider, irregular ER enlargements are formed by the expression of the N-terminal region of 27γz in Arabidopsis, but these have homogeneous electron density, with no signs of filaments (Geli *et al.*, 1994). PBs formed by chimeric fusions containing spider elastin-like polypeptides can have a loosely

packed content, but they are round and rarely larger than 3  $\mu\text{m}$ , with no well-defined filaments (Conley *et al.*, 2009; Phan *et al.*, 2014). Thus, the unusual structures that we found formed by 16 $\gamma$ zf markedly differed from 27 $\gamma$ zf PBs and from ER enlargements formed by various other storage proteins at early stages of seed development or by protein fusions that polymerize in the ER.

However, 16 $\gamma$ zf threads strikingly resemble those formed by diabetes insipidus-inducing mutants of the antidiuretic hormone arginine vasopressin precursor (Birk *et al.*, 2009; Beuret *et al.*, 2017). These dominant mutations can be in different locations along the precursor, but they all result in abnormal inter-chain disulfide bonds leading to oligomerization and, in some cases, partial resistance to denaturation by SDS/reducing agent, whereas the normal precursor has eight intra-chain bonds. The misfolded precursors thus accumulate in the ER instead of trafficking to secretory granules and form irregularly packed electron-dense filaments, which in some cases coalesce in more uniformly electron-dense regions, similar to 16 $\gamma$ zf. Although the mutated precursors seem unable to form canonical amyloid cross- $\beta$ -sheets, their ability to form fibers resembles amyloid aggregation (Beuret *et al.*, 2017).

Our results indicated that 16 $\gamma$ zf was not a structurally defective protein rapidly degraded by ER quality control. 16 $\gamma$ zf threads were disulfide-bonded polymers that remained partially soluble in oxidizing conditions, unlike 27 $\gamma$ zf polymers. Only when the two recombinant zeins were co-expressed, 16 $\gamma$ zf become fully insoluble unless reduced, indicating direct interactions with 27 $\gamma$ zf. 16 $\gamma$ z present in natural maize PBs was in part solubilized by alcohol together with  $\alpha$ -zeins, but no alcohol-soluble 16 $\gamma$ zf was detected in transgenic Arabidopsis or upon transient co-expression with 27 $\gamma$ zf. This supports the hypothesis that, in maize, at least one of the alcohol-soluble  $\alpha$ -zeins directly interacts with 16 $\gamma$ z, consistent with the location of 16 $\gamma$ z in natural PBs (Lending and Larkins, 1989; Yao *et al.*, 2016) and the results of yeast two-hybrid assays (Kim *et al.*, 2002, 2006). A specific role of 16 $\gamma$ z in natural, heterotypic PB assembly is also supported by the characteristics of two maize mutations with opaque endosperm, *mucronate* and *opaque10*. *mucronate* is a frameshift mutation that completely changes the 16 $\gamma$ z sequence for the last 63 amino acids, abolishes its solubility in 70% ethanol supplemented with 2-ME, and markedly weakens the interaction with 22-kD  $\alpha$ -zein (Kim *et al.*, 2006). In *mucronate* seeds, the overall amount of zeins is reduced (Salamini *et al.*, 1983) and PBs have angular deformations that often interrupt the outer layer, indicating defects in the organization of the interface between  $\alpha$ - and  $\gamma$ -zeins (Zhang and Boston, 1992). *opaque10* is a frameshift mutation generating a premature stop codon in a cereal-specific protein located in PBs (Yao *et al.*, 2016). *opaque10* PBs are misshaped and often irregularly elongated. The ordered localizations of 16 $\gamma$ z and of the 22-kD  $\alpha$ -zein that is normally located next to it are disrupted, and the two zeins are dispersed in the PB (Yao *et al.*, 2016). RNAi, used to inhibit the synthesis of  $\gamma$ -zeins in maize, also causes PB misshaping and angular deformations (Wu and Messing, 2010). A specific role of 16 $\gamma$ z could not be established in this case, since the synthesis of both the 27- and 16-kD polypeptides was almost fully inhibited. However,

RNAi in which the synthesis of 16 $\gamma$ z, 50 $\gamma$ z, and  $\beta$ -zein was concomitantly suppressed indicated that these proteins are mainly involved in PB expansion, whereas 27 $\gamma$ -zein controls PB initiation and shape, consistent with our data in transgenic Arabidopsis (Guo *et al.*, 2013).

Sorghum (*Sorghum bicolor*), a very close relative of maize (Swigoňová *et al.*, 2004), has not undergone WGD and contains only two genes belonging to the same prolamin II group of  $\gamma$ -zeins, *kafirin2 $\gamma$ 27* and *kafirin2 $\gamma$ 50* (Belton *et al.*, 2006; Xu and Messing, 2009), and is therefore lacking a 16 $\gamma$ z orthologue. Similar to  $\beta$ - and  $\gamma$ -zeins,  $\beta$ - and  $\gamma$ -kafirins form the more electron-dense structures of the PB; however, these are not limited to the PB periphery and are also concentrated in the central core or form patches within the less-dense regions (Shull *et al.*, 1992). This lack of organization in layers with clear boundaries between dense and less-dense regions (the latter mainly containing  $\alpha$ -type prolamins), compared to maize PBs may thus be related to the absence of a 16 $\gamma$ z-like prolamin.

Our domain-exchange results suggested that the different behavior of the two  $\gamma$ -zeins was mainly due to their N-terminal domains. A synthetic version of the (VHLPPP)<sub>8</sub> repeated segment has an amphipathic polyproline II structure and *in vitro* affinity to liposomes that partially mimics the lipid composition of the plant ER, suggesting that the repeat may favor interaction of 27 $\gamma$ z with the inner surface of the ER membrane (Kogan *et al.*, 2004). The Zera sequence is a 27 $\gamma$ z portion almost identical to the one used to construct zeolin and, like zeolin, it determines PB formation in a Cys-dependent fashion when fused to a number of proteins (Torrent *et al.*, 2009). In a Zera-fluorescent protein fusion, progressive deletion of the Pro-rich hexapeptides leads to progressively increased secretion and reduced PB size but does not alter their spherical shape (Llop-Tous *et al.*, 2010), indicating that the peculiar structures formed by 16 $\gamma$ z are not simply due to the loss of repeats. Indeed, the N-terminal region of 16 $\gamma$ z has also lost three Cys residues and contains two degenerated Pro-rich sequences containing two new Tyr residues—aromatic amino acids inhibit the formation of polyproline II helices (Brown and Zondlo, 2012)—as well as other aromatic amino acids and a new Gln-rich short sequence (Fig. 1). In combination, these features may have abolished the ability to interact orderly with lipids and determined the formation of rod-like polymers involved in stabilizing the  $\gamma$ -zein/ $\alpha$ -zein interface.

Proteins containing disulfide bonds generally have higher evolutionary rates (Feyertag and Alvarez-Ponce, 2017). Intra-chain disulfides probably stabilize important conformations and thus have a buffering, chaperone-like effect that makes the polypeptide more tolerant to mutations; thus, once acquired, inter-chain disulfides are rarely changed (Wong *et al.*, 2011; Feyertag and Alvarez-Ponce, 2017). Unpaired Cys residues are also relatively more conserved than other amino acids (Wong *et al.*, 2011). The major deletion and the mutations generating 16 $\gamma$ z have eliminated a number of 27 $\gamma$ z cysteine residues and have altered the biochemical and polymerization properties of the prolamin, but they have not caused gross misfolding and degradation by quality control. They have instead promoted a new role of the protein and a new PB organization.

Prolamins form peculiar heteropolymers. Analysis of many prolamin polypeptides and their positioning within a PB in different grasses indicates that a high genetic variability is tolerated, probably because PB function is simply constituted by the high accumulation of reduced nitrogen in the first compartment of the secretory pathway. However, within an individual species, certain requirements for optimal PB assembly exist, as indicated by the many natural and artificial cereal mutants analysed. We have shown here that an apparently defective zein polypeptide, generated upon maize whole-genome duplication, forms very unusual structures that may explain its specific structural role at the interface between the ancient and the more recently evolved maize prolamins. The organization of 16 $\gamma$ z structures resembles abnormally disulfide-linked, amyloid-like fibers formed by pathological mutants of a human hormone precursor. It thus appears that mutations giving rise to similar abnormal structures within the ER can result in pathogenic loss of function in one case but can be exploited in a developmental process in another.

## Supplementary data

Supplementary data are available at JXB online.

Fig. S1. Identities of the major polypeptides present in purified maize PBs, as determined by LC-ESI-MS/MS analysis (including the protocol for protein in-gel digestion and the analysis).

Fig. S2. Variability in denaturation-resistant oligomers.

Fig. S3. Dilated ER in leaf cells of transgenic *Arabidopsis* expressing 16 $\gamma$ zf.

Table S1. Peptide identification by LC-ESI-MS/MS analysis, and protein assignment.

## Acknowledgments

This work was supported by the Project 'Risorse biologiche e tecnologie innovative per lo sviluppo sostenibile del sistema agroalimentare' and Project 'Filagro - Strategie innovative e sostenibili per la filiera agroalimentare' of the 2006 and 2012 Agreements between Regione Lombardia and CNR (to EP and AV).

## Author Contributions

D. Mainieri, EP, ES, and AV designed the research; D. Mainieri, CAM, BP, D. Maffi, MT, LE, FF, EP, and AV performed the experiments; ES, FF, EP, and AV wrote the manuscript.

## References

- Arcalis E, Stadtmann J, Marcel S, Drakakaki G, Winter V, Rodriguez J, Fischer R, Altmann F, Stoger E.** 2010. The changing fate of a secretory glycoprotein in developing maize endosperm. *Plant Physiology* **153**, 693–702.
- Bagga S, Adams H, Kemp JD, Sengupta-Gopalan C.** 1995. Accumulation of 15-kilodalton zein in novel protein bodies in transgenic tobacco. *Plant Physiology* **107**, 13–23.
- Belton PS, Delgadillo I, Halford NG, Shewry PR.** 2006. Kafirin structure and functionality. *Journal of Cereal Science* **44**, 272–286.
- Beuret N, Hasler F, Prescianotto-Baschong C, Birk J, Rutishauser J, Spiess M.** 2017. Amyloid-like aggregation of provasopressin in diabetes insipidus and secretory granule sorting. *BMC Biology* **15**, 5.
- Birk J, Friberg MA, Prescianotto-Baschong C, Spiess M, Rutishauser J.** 2009. Dominant pro-vasopressin mutants that cause diabetes insipidus form disulfide-linked fibrillar aggregates in the endoplasmic reticulum. *Journal of Cell Science* **122**, 3994–4002.
- Brown AM, Zondlo NJ.** 2012. A propensity scale for type II polyproline helices (PPII): aromatic amino acids in proline-rich sequences strongly disfavor PPII due to proline–aromatic interactions. *Biochemistry* **51**, 5041–5051.
- Chapman BA, Bowers JE, Feltus FA, Paterson AH.** 2006. Buffering of crucial functions by paleologous duplicated genes may contribute cyclicity to angiosperm genome duplication. *Proceedings of the National Academy of Sciences, USA* **103**, 2730–2735.
- Clough SJ, Bent AF.** 1998. Floral dip: a simplified method for *Agrobacterium*-mediated transformation of *Arabidopsis thaliana*. *The Plant Journal* **16**, 735–743.
- Coleman CE, Herman EM, Takasaki K, Larkins BA.** 1996. The maize gamma-zein sequesters alpha-zein and stabilizes its accumulation in protein bodies of transgenic tobacco endosperm. *The Plant Cell* **8**, 2335–2345.
- Conley AJ, Joensuu JJ, Menassa R, Brandle JE.** 2009. Induction of protein body formation in plant leaves by elastin-like polypeptide fusions. *BMC Biology* **7**, 48.
- de Virgilio M, De Marchis F, Bellucci M, Mainieri D, Rossi M, Benvenuto E, Arcioni S, Vitale A.** 2008. The human immunodeficiency virus antigen Nef forms protein bodies in leaves of transgenic tobacco when fused to zeolin. *Journal of Experimental Botany* **59**, 2815–2829.
- Ems-McClung SC, Benmoussa M, Hainline BE.** 2002. Mutational analysis of the maize gamma zein C-terminal cysteine residues. *Plant Science* **162**, 131–141.
- Faoro F, Tornaghi R, Belli G.** 1991. Localization of the Closteroviruses on grapevine thin sections and their identification by immunogold labelling. *Journal of Phytopathology* **133**, 297–306.
- Feyertag F, Alvarez-Ponce D.** 2017. Disulfide bonds enable accelerated protein evolution. *Molecular Biology and Evolution* **34**, 1833–1837.
- Geli MI, Torrent M, Ludevid D.** 1994. Two structural domains mediate two sequential events in [gamma]-zein targeting: protein endoplasmic reticulum retention and protein body formation. *The Plant Cell* **6**, 1911–1922.
- Gomez-Navarro N, Miller E.** 2016. Protein sorting at the ER–Golgi interface. *The Journal of Cell Biology* **215**, 769–778.
- Gu YQ, Wanjigi H, Coleman-Derr D, Kong X, Anderson OD.** 2010. Conserved globulin gene across eight grass genomes identify fundamental units of the loci encoding seed storage proteins. *Functional & Integrative Genomics* **10**, 111–122.
- Guo X, Yuan L, Chen H, Sato SJ, Clemente TE, Holding DR.** 2013. Nonredundant function of zeins and their correct stoichiometric ratio drive protein body formation in maize endosperm. *Plant Physiology* **162**, 1359–1369.
- Jiao Y, Wickett NJ, Ayyampalayam S, et al.** 2011. Ancestral polyploidy in seed plants and angiosperms. *Nature* **473**, 97–100.
- Kassahn KS, Dang VT, Wilkins SJ, Perkins AC, Ragan MA.** 2009. Evolution of gene function and regulatory control after whole-genome duplication: comparative analyses in vertebrates. *Genome Research* **19**, 1404–1418.
- Kawagoe Y, Suzuki K, Tasaki M, Yasuda H, Akagi K, Katoh E, Nishizawa NK, Ogawa M, Takaiwa F.** 2005. The critical role of disulfide bond formation in protein sorting in the endosperm of rice. *The Plant Cell* **17**, 1141–1153.
- Kim CS, Gibbon BC, Gillikin JW, Larkins BA, Boston RS, Jung R.** 2006. The maize *Mucronate* mutation is a deletion in the 16-kDa  $\gamma$ -zein gene that induces the unfolded protein response. *The Plant Journal* **48**, 440–451.
- Kim CS, Woo YM YM, Clore AM, Burnett RJ, Carneiro NP, Larkins BA.** 2002. Zein protein interactions, rather than the asymmetric distribution of zein mRNAs on endoplasmic reticulum membranes, influence protein body formation in maize endosperm. *The Plant Cell* **14**, 655–672.
- Klein EM, Mascheroni L, Pompa A, Ragni L, Weimar T, Lilley KS, Dupree P, Vitale A.** 2006. Plant endoplasmic supports the protein

- secretory pathway and has a role in proliferating tissues. *The Plant Journal* **48**, 657–673.
- Kogan MJ, López O, Cocera M, López-Iglesias C, De La Maza A, Giralt E.** 2004. Exploring the interaction of the surfactant N-terminal domain of  $\gamma$ -Zein with soybean phosphatidylcholine liposomes. *Biopolymers* **73**, 258–268.
- Larkins BA, Hurkman WJ.** 1978. Synthesis and deposition of zein in protein bodies of maize endosperm. *Plant Physiology* **62**, 256–263.
- Lending CR, Larkins BA.** 1989. Changes in the zein composition of protein bodies during maize endosperm development. *The Plant Cell* **1**, 1011–1023.
- Llop-Tous I, Madurga S, Giralt E, Marzabal P, Torrent M, Ludevid MD.** 2010. Relevant elements of a maize  $\gamma$ -zein domain involved in protein body biogenesis. *The Journal of Biological Chemistry* **285**, 35633–35644.
- Mainieri D, Morandini F, Maîtrejean M, Saccani A, Pedrazzini E, Alessandro V.** 2014. Protein body formation in the endoplasmic reticulum as an evolution of storage protein sorting to vacuoles: insights from maize  $\gamma$ -zein. *Frontiers in Plant Science* **5**, 331.
- Mainieri D, Rossi M, Archinti M, Bellucci M, De Marchis F, Vavassori S, Pompa A, Arcioni S, Vitale A.** 2004. Zeolin. A new recombinant storage protein constructed using maize  $\gamma$ -zein and bean phaseolin. *Plant Physiology* **136**, 3447–3456.
- Misra PS, Mertz ET, Glover DV.** 1976. Studies on corn proteins. IX. Comparison of the amino acid composition of Landry-Moureaux and Paulis-Wall endosperm fractions. *Cereal Chemistry* **53**, 699–704.
- Muench DG, Chuong SD, Franceschi VR, Okita TW.** 2000. Developing prolamine protein bodies are associated with the cortical cytoskeleton in rice endosperm cells. *Planta* **211**, 227–238.
- Pedrazzini E, Mainieri D, Marrano CA, Vitale A.** 2016. Where do protein bodies of cereal seeds come from? *Frontiers in Plant Science* **7**, 1139.
- Phan HT, Hause B, Hause G, Arcalis E, Stoger E, Maresch D, Altmann F, Joensuu J, Conrad U.** 2014. Influence of elastin-like polypeptide and hydrophobin on recombinant hemagglutinin accumulations in transgenic tobacco plants. *PLoS ONE* **9**, e99347.
- Pompa A, Vitale A.** 2006. Retention of a bean phaseolin/maize  $\gamma$ -Zein fusion in the endoplasmic reticulum depends on disulfide bond formation. *The Plant Cell* **18**, 2608–2621.
- Prat S, Cortadas J, Puigdomènech P, Palau J.** 1985. Nucleic acid (cDNA) and amino acid sequences of the maize endosperm protein glutelin-2. *Nucleic Acids Research* **13**, 1493–1504.
- Prat S, Pérez-Grau L, Puigdomènech P.** 1987. Multiple variability in the sequence of a family of maize endosperm proteins. *Gene* **52**, 41–49.
- Reyes FC, Chung T, Holding D, Jung R, Vierstra R, Otegui MS.** 2011. Delivery of prolamins to the protein storage vacuole in maize aleurone cells. *The Plant Cell* **23**, 769–784.
- Saito Y, Kishida K, Takata K, Takahashi H, Shimada T, Tanaka K, Morita S, Satoh S, Masumura T.** 2009. A green fluorescent protein fused to rice prolamin forms protein body-like structures in transgenic rice. *Journal of Experimental Botany* **60**, 615–627.
- Saito Y, Shigemitsu T, Yamasaki R, et al.** 2012. Formation mechanism of the internal structure of type I protein bodies in rice endosperm: relationship between the localization of prolamin species and the expression of individual genes. *The Plant Journal* **70**, 1043–1055.
- Salamini F, Di Fonzo N, Fornasari E, Gentinetta E, Reggiani R, Soave C.** 1983. *Mucronate*, *Mc*, a dominant gene of maize which interacts with *opaque-2* to suppress zein synthesis. *Theoretical and Applied Genetics* **65**, 123–128.
- Shewry PR, Halford NG.** 2002. Cereal seed storage proteins: structures, properties and role in grain utilization. *Journal of Experimental Botany* **53**, 947–958.
- Shull JM, Watterson JJ, Kirleis AW.** 1992. Purification and immunocytochemical localization of kafirins in *Sorghum bicolor* (L. Moench) endosperm. *Protoplasma* **171**, 64–74.
- Swigoňová Z, Lai J, Ma J, Ramakrishna W, Llaca V, Bennetzen JL, Messing J.** 2004. Close split of sorghum and maize genome progenitors. *Genome Research* **14**, 1916–1923.
- Torrent M, Llompart B, Lasserre-Ramassamy S, Llop-Tous I, Bastida M, Marzabal P, Westerholm-Parvinen A, Saloheimo M, Heifetz PB, Ludevid MD.** 2009. Eukaryotic protein production in designed storage organelles. *BMC Biology* **7**, 5.
- Vitale A, Smaniotti E, Longhi R, Galante E.** 1982. Reduced soluble proteins associated with maize endosperm protein bodies. *Journal of Experimental Botany* **33**, 439–448.
- Wang J, Shen J, Cai Y, Robinson DG, Jiang L.** 2013. Successful transport to the vacuole of heterologously expressed mung bean 8S globulin occurs in seed but not in vegetative tissues. *Journal of Experimental Botany* **64**, 1587–1601.
- Washida H, Sugino A, Messing J, Esen A, Okita TW.** 2004. Asymmetric localization of seed storage protein RNAs to distinct subdomains of the endoplasmic reticulum in developing maize endosperm cells. *Plant & Cell Physiology* **45**, 1830–1837.
- Wong JW, Ho SY, Hogg PJ.** 2011. Disulfide bond acquisition through eukaryotic protein evolution. *Molecular Biology and Evolution* **28**, 327–334.
- Woo YM, Hu DW, Larkins BA, Jung R.** 2001. Genomics analysis of genes expressed in maize endosperm identifies novel seed proteins and clarifies patterns of zein gene expression. *The Plant Cell* **13**, 2297–2317.
- Wu Y, Messing J.** 2010. RNA interference-mediated change in protein body morphology and seed opacity through loss of different zein proteins. *Plant Physiology* **153**, 337–347.
- Xu J-H, Messing J.** 2008. Organization of the prolamin gene family provides insight into the evolution of the maize genome and gene duplications in grass species. *Proceedings of the National Academy of Sciences, USA* **105**, 14330–14335.
- Xu J-H, Messing J.** 2009. Amplification of prolamin storage protein genes in different subfamilies of the Poaceae. *Theoretical and Applied Genetics* **119**, 1397–1412.
- Yamagata T, Kato H, Kuroda S, Abe S, Davies E.** 2003. Uncleaved legumin in developing maize endosperm: identification, accumulation and putative subcellular localization. *Journal of Experimental Botany* **54**, 913–922.
- Yao D, Qi W, Li X, Yang Q, Yan S, Ling H, Wang G, Wang G, Song R.** 2016. Maize *opaque10* encodes a cereal-specific protein that is essential for the proper distribution of zeins in endosperm protein bodies. *PLoS Genetics* **12**, e1006270.
- Yu M, Lau TY, Carr SA, Krieger M.** 2012. Contributions of a disulfide bond and a reduced cysteine side chain to the intrinsic activity of the high-density lipoprotein receptor SR-BI. *Biochemistry* **51**, 10044–10055.
- Zhang F, Boston RS.** 1992. Increases in binding protein (BiP) accompany changes in protein body morphology in three high-lysine mutants of maize. *Protoplasma* **171**, 142–152.